*International Geology Review*, Vol. 49, 2007, p. 416–430.


# Significance of the Ca-Na Pyroxene-Lawsonite-Chlorite Assemblage in Blueschist-Facies Metabasalts: An Example from the Renge Metamorphic Rocks, Southwest Japan

T. TSUJIMORI[1] AND J. G. LIOU

*Department of Geological and Environmental Sciences, Stanford University, Stanford, California 94305-2115*

## Abstract

Paleozoic lawsonite-bearing low-grade metabasalts with rare flattened pillow structures occur in the Chugoku Mountains, Southwest Japan. The meta-mafic rocks are divided into meta-pillow basalt core (PBC), meta-pillow basalt rim (PBR), and metabasaltic breccia (BB). The PBC have MORB-like major and trace element concentrations, contain 5 wt% water, and a Na-amphibole–free mineral assemblage: Ca-Na pyroxene (maximum 29% jadeite component) + lawsonite + chlorite + quartz. In contrast, the PBR and BB contain a lawsonite-blueschist–facies mineral assemblage: Na-amphibole ± lawsonite + pumpellyite ± chlorite + albite + quartz. Parageneses and compositions of minerals yield equilibrium P-T conditions of T< 280°C and P = 0.6–0.7 GPa for all three rock types. Phase relations in the 2Al–Ca–2$Fe^{3+}$–(Fe+Mg) tetrahedron suggest that the Na–amphibole-free mineral assemblage in PBC occurs only under relatively oxidized conditions. This mineral assemblage has been described from low-grade metabasalts in several high-P–low-T terranes, and might be a low-T equivalent of the lawsonite eclogite mineral assemblage. We propose that interaction of fluids with subducting old oceanic crust first produces the Ca-Na pyroxene + lawsonite + chlorite assemblage by hydration reactions at shallow depths in a cold subduction zone. With subduction to greater depths, such intensely hydrated metabasalts with the Na-amphibole-free mineral assemblage transforms to lawsonite eclogite below 300°C.

## Introduction

LAWSONITE, $CaAl_2Si_2O_7(OH)_2 \cdot H_2O$, is an index mineral for high-P–low-T (HP-LT) blueschist and eclogite-facies mafic rocks. Nitsch (1968) and Liou (1971) independently determined the minimum pressure stability of lawsonite to be P = ~0.3 GPa at T = ~300°C by a decompression reaction of laumontite to lawsonite + quartz + $H_2O$. After these early experiments, subsequent experimental studies revealed the upper pressure stability of lawsonite up to 8–10 GPa at temperatures of 750–900°C (Pawley, 1994; Schmidt and Poli, 1994; Schmidt, 1995; Okamoto and Maruyama, 1999). Consequently, lawsonite has been considered as the most important hydrous mineral in the recycling of volatiles and selective trace elements in a subduction zone and the cooling history of the Earth (Schmidt and Poli, 1998; Maruyama and Liou, 2005; Ohtani, 2005; Tsujimori et al., 2006b). Recently, petrologic characteristics of natural lawsonite-eclogites containing the mineral assemblage garnet + omphacite + lawsonite (Tsujimori et al., 2006b) have been documented from both regional HP-LT terranes (e.g., Zack et al., 2004; Tsujimori et al., 2005, 2006a) and ultrahigh-pressure (UHP) xenoliths (e.g., Usui et al., 2003, 2006). In both cases, however, the early process prior to lawsonite eclogitization of subducting oceanic crust is not clear. Specifically, what is the precursor mineral assemblage for lawsonite-eclogites? In this paper, we describe petrologic and mineralogic characteristics of low-T metabasalt and associated blueschist-facies mafic rocks in the Chugoku Mountains, SW Japan, and suggest that the mineral assemblage Ca-Na pyroxene + lawsonite + chlorite (Okay, 1982; Hirajima, 1983; Sakakibara, 1991) of the low-T blueschist-facies metabasalt is the most likely candidate, in which chlorite decomposes to produce garnet with increasing pressure and temperature.[2]

[1]Corresponding author. Present address: Pheasant Memorial Laboratory for Geochemistry and Cosmochemistry, Institute for Study of the Earth's Interior, Okayama University, Misasa, Tottori 682-0193 Japan; email: tatsukix@misasa.okayama-u.ac.jp

[2]Mineral abbreviations are after Kretz (1983); we also use Ca-Na pyroxene (Ca-Na px), aegirine (Ae), Na amphibole (Na-amp), phengite (Phe), and stilpnomelane (Stp) throughout this paper.

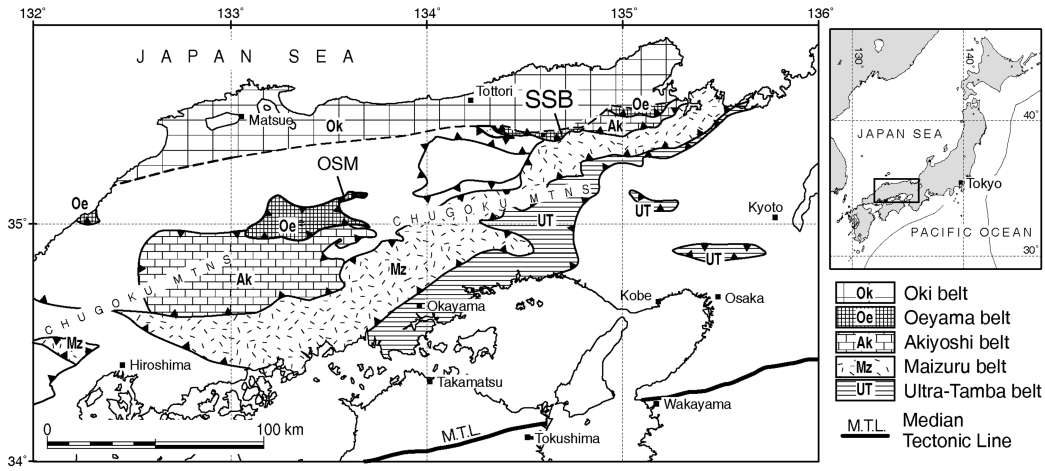


FIG. 1. Simplified map of the Chugoku Mountains, showing various petrotectonic units and the sampling locality in the Sekinomiya serpentinite body (SSB). Modified after Tsujimori and Liou (2005a).

## Geologic Outline

In the Chugoku Mountains, Pre-Triassic rocks occur in the Oki, Oeyama, Akiyoshi, Maizuru, and Ultra-Tamba belts. These geotectonic units tectonically underlie nearly E-W–trending Paleozoic ophiolites and accretionary complexes (e.g., Isozaki, 1997; Ishiwatari and Tsujimori, 2003; Fig. 1). A few blueschist localities have been identified in serpentinized peridotite bodies of the early Paleozoic Oeyama belt; phengites from blueschist-facies metapelite yield K-Ar ages of 330–280 Ma (Nishimura, 1998; Tsujimori and Itaya, 1999). In this study, several lawsonite-bearing metabasalts were collected at an outcrop (6 × 5 m) of a blueschist-bearing HP block exposed in the Paleozoic schist locality along the southwestern margin of the Sekinomiya serpentinite body (SSB) in the eastern Chugoku Mountains (Fig. 1); the SSB is the largest (20 × 5 km) serpentinized peridotite body of the Oeyama belt (Ishiwatari and Hayasaka, 1992). Lawsonite blueschist and rare jadeitite occur as tectonic blocks along the southern margin of the SSB (Hashimoto and Igi, 1970; Tazaki and Ishiuchi, 1976); the blueschist-and jadeitite-bearing serpentinite mélange unit of the SSB is similar to the Osayama serpentinite mélange (OSM in Fig. 1) located about 150 km west of the studied area (Tsujimori, 1997, 1998; Tsujimori and Itaya, 1999; Tsujimori and Liou, 2004, 2005a, 2005b; Tsujimori et al., 2005).

In outcrop, lawsonite-bearing metabasalts exhibiting rare flattened pillow structures are interlayered with metabasaltic breccia, meta-chert, and marble layers < 1.5 m thick. Meta-pillow basalt is weakly foliated and consists of rare Na-amphibole–bearing bluish rims (1 to 5 cm wide) and dark greenish cores with a Ca-Na pyroxene-lawsonite-chlorite assemblage. In contrast, basaltic breccia is moderately foliated fine-grained blueschist.

## Petrography

### *Meta-pillow basalt core (PBC)*

The PBC is fine-grained and well-recrystallized except for minor relict igneous augite; rare lawsonite pseudomorphs after plagioclase are present (Figs. 2A and 2B). The mineral assemblage consists mainly of Ca–Na pyroxene, lawsonite, and chlorite, with minor titanite, relict igneous augite, and quartz. Some quartz-lawsonite veins (2–15 mm) (Fig. 3) cross-cut the matrix; the matrix contains Ca–Na-px + Lws + Chl and minor quartz and titanite (Fig. 2C). Yellow to pale green pleochroic Ca-Na pyroxene occurs as irregularly shaped fibrous aggregates (<0.2 mm) of tiny crystals, discrete prismatic crystals (<0.05 mm), and replacements of relict igneous augite. Augite occurs as colorless subhedral to euhedral crystals (0.3–0.5 mm). Except for the replacements of relict augite, Ca-Na pyroxene commonly coexists with quartz. Lawsonite occurs as elongate prisms (<0.1 mm) or as aggregates in the matrix; relatively large euhedral crystals (maximum 0.5 mm) occur in quartz-lawsonite veins. Some lawsonite contains submicron iron oxide inclusions,

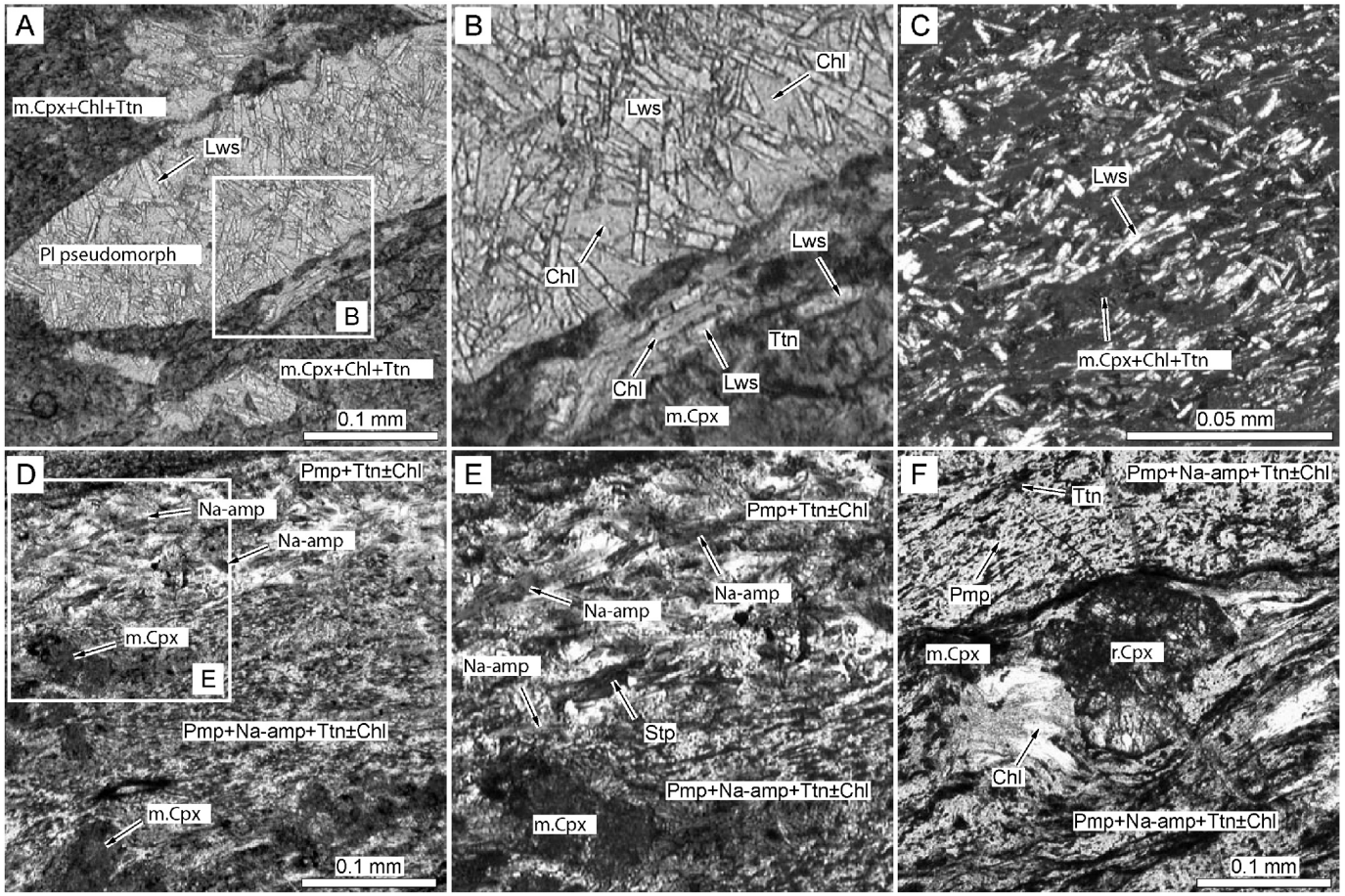


FIG. 2. Photomicrographs of meta-pillow basalts from Sekinomiya serpentinite body. A. A pseudomorph after igneous plagioclase consisting of lawsonite and chlorite in meta-pillow basalt core. PPL = plane polarized light. B. Enlarged view of a part of A showing a boundary between the pseudomorph and fine-grained matrix, PPL. C. Ca-Na pyroxene–bearing fine-grained matrix of a PBC. XPL = crossed polarized light. D. Na-amphibole–bearing matrix of meta-pillow basalt rim, PPL. E. Enlarged view of a part of D. F. Relict igneous augite in PBR, PPL.

probably magnetite. Polycrystalline chlorite coexists with all other minerals.

*Meta-pillow basalt rim (PBR)*

The PBR occurs in 1–5 cm thick pillow rims, and consists mainly of pumpellyite and Na-amphibole, with minor titanite, stilpnomelane, quartz and albite (Figs. 2D and 2E), rare lawsonite, Ca-Na pyroxene, and relict augite (Fig. 2F). Na-amphibole occurs as discrete prisms (< 0.2 mm in length) and shows slight color zonation from deep blue at the cores to pale blue at the rims. Pumpellyite occurs as irregular aggregates of tiny crystals or radial aggregates of acicular crystals. In the PBR, Ca-Na pyroxene replacing relict augite does not coexist with quartz.

*Meta-basaltic breccia (BB)*

The BB consists of heterogeneous, moderately foliated rocks. The mineral assemblage consists mainly of Na-amphibole, lawsonite, pumpellyite, chlorite, and albite, with minor quartz and titanite; a penetrative schistosity is defined by preferred orientation of Na-amphibole and lawsonite. Rare phengite, stilpnomelane, and K-feldspar occur as accessories. A few relict clastic augite grains have persisted. Na-amphibole occurs as fine-grained bundle aggregates, lawsonite as elongated prisms (<0.05 mm in length), and pumpellyite as aggregates of tiny crystals. BB is characterized by the assemblage Na-amp + Lws + Pmp + Chl, with albite, quartz, and titanite in excess.

## Bulk-Rock Compositions

Concentrations of major (Si, Ti, Al, Fe, Mn, Mg, Ca, Na, K, and P) and trace elements (Ni, Cu, Zn, Pb, Y, and V) were analyzed with a Rigaku System 3270 X-ray fluorescence spectrometer at Kanazawa University. The operating conditions for both major and trace elements were 50 kV accelerating voltage and 20 mA beam current. Other trace elements (Sc, Cr, Co, Rb, Sr, Zr, Nb, Ba, La, Ce, Pb, Sm, Eu, Yb, Lu, Hf, and Th) were determined by instrumental neutron activation analysis (INAA). The INAA samples were activated at Kyoto University Reactor, and the gamma-ray spectroscopic analyses were done at the Radioisotope Laboratory of Kanazawa University.

Representative PBC, PBR, and BB bulk-rock analyses are listed in Table 1. The three rock types have mafic compositions with $SiO_2$ = 47.0–52.7 wt%, $Al_2O_3$= 14.2–15.6 wt%, FeO* = 11.3–12.6

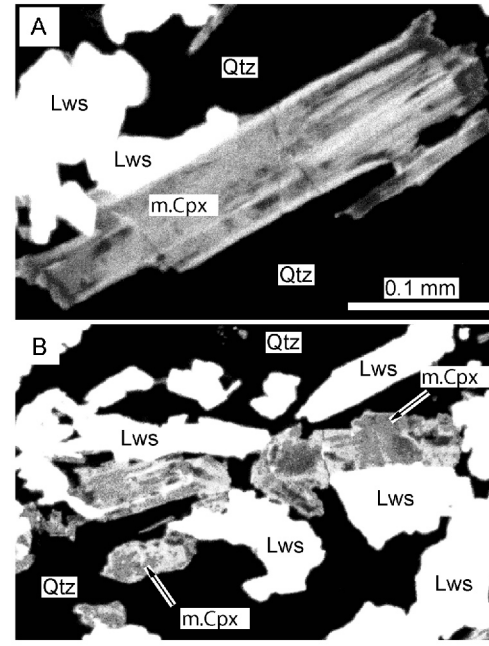


FIG. 3. X-ray images of Al concentration showing occurrences and internal textures of Ca–Na pyroxenes in quartz-lawsonite veins of the meta-pillow basalt core; brighter shades indicate higher Al content (jadeite component). A. A crystal nearly parallel to the crystallographic *c*-axis. B. Crystals oblique to the *c*-axis.

and $TiO_2$ = 1.6–1.8 wt%, and variable water content based on the LOI (loss-on-ignition): PBC (5.0 wt%), PBR (2.7 wt%), and BB (3.3 wt%). Water contents up to 5 wt% are comparable with calculated $H_2O$ content in blueschist-facies MORB (Hacker et al., 2003). PBC is richer in MgO (6.5 wt%) than the PBR (4.0 wt.%) and BB (4.2 wt%). The PBR has higher CaO (12.7 wt%) than the PMC (8.8 wt%) and BB (5.2 wt%); this suggests Ca-metasomatism during hydrothermal alteration was more severe at the pillow rim. The BB contains higher $Na_2O$ (3.6 wt%) than the PMC (2.7 wt%) and PMR (2.8 wt%); the enrichment in Na suggests that the degree of seawater alteration might have been higher in the breccia. The pillow basalts are characterized by significantly higher Cr (109–131 ppm) and Ni (56–81 ppm), and lower Ba (78–124 ppm) than basaltic breccia (Table 1). In a spider diagram (Sun and McDonough, 1989) N-MORB for normalization: Fig. 4A), the PBC and BB show a trend similar to those of Sambagawa mafic schists (Okamoto et al., 1999). Nearly flat chondrite-normalized REE patterns (Sun

TABLE 1. Bulk-Rock Compositions of Representative Rock Types of the Investigated Samples

| Rock type | PBC | PBR | BB |
|---|---|---|---|
| Major-element compositions wt% | | | |
| $SiO_2$ | 46.98 | 49.10 | 52.71 |
| $TiO_2$ | 1.68 | 1.58 | 1.75 |
| $Al_2O_3$ | 14.38 | 14.23 | 15.63 |
| FeO[1] | 12.78 | 11.64 | 11.29 |
| MnO | 0.18 | 0.25 | 0.18 |
| MgO | 6.50 | 4.00 | 4.17 |
| CaO | 8.82 | 12.70 | 5.22 |
| $Na_2O$ | 2.66 | 2.79 | 3.62 |
| $K_2O$ | 0.92 | 0.27 | 1.82 |
| $P_2O_5$ | 0.19 | 0.26 | 0.22 |
| L.O.I. ($H_2O$) | 5.03 | 2.70 | 3.30 |
| Total | 100.12 | 99.52 | 99.91 |
| Trace-element compositions, ppm | | | |
| Sc | 43.6 | 34.2 | |
| Cr | 109 | 131 | 25 |
| Co | 52 | 57 | 41 |
| Ni | 56 | 81 | 25 |
| Cu | 78 | 27 | 34 |
| Zn | 118 | 93 | 123 |
| Rb | 23 | 7 | 45 |
| Sr | 120 | 65 | 129 |
| Y | 42 | 68 | 53 |
| V | 332 | 301 | 335 |
| Zr | 111 | 136 | 162 |
| Nb | 8 | 10 | 3 |
| Pb | | 4 | 7 |
| Ba | 124 | 78 | 251 |
| La | 5.0 | 10.4 | |
| Ce | 20.9 | 27.8 | |
| Sm | 3.8 | 6.2 | |
| Eu | 1.4 | 1.9 | |
| Yb | 4.8 | 6.7 | |
| Lu | 0.5 | 0.7 | |
| Hf | 1.3 | 3.1 | |
| Th | 0.6 | | |

[1]Total Fe as FeO.

and McDonough, 1989; Fig. 4B) and relationships of Zr (111–136 ppm)–Zr/Yi (2–3) and Nb/Y (0.1–0.2)–Ti/Y (139–240) suggest a MORB-like affinity for the pillow basalts (Pearce, 1982, 1983); new discrimination schemes by Vermeesch (2006a, 2006b) and Snow (2006) also suggest a MORB origin.

## Mineral Chemistry

Electron microprobe (EMP) analysis and X-ray element mapping were carried out with a JEOL JXA-8800R EMP at Kanazawa University and a JEOL JXA-8900R EMP at Okayama University of Science. Quantitative analyses were performed with 15 kV accelerating voltage, 12 nA beam current, and 3–5 μm beam size. Natural and synthetic silicates and oxides were used for standards. The ZAF method (oxide basis) was employed for matrix corrections. In this study, the presence of quartz was identified by X-ray mapping. Representative EMP analyses are listed in Table 2; Fe was assumed to be $Fe^{2+}$ unless otherwise noted.

### *Metamorphic clinopyroxenes*

Figure 5 shows compositions of metamorphic clinopyroxenes from each rock type; the $Fe^{2+}/Fe^{3+}$ ratio and end-member components were calculated following Harlow (1999). Two metamorphic pyroxenes, aegirine-augite and diopsidic pyroxene, are common in the PBC. Aegirine-augite is $jd_{7-29}di + hd_{21-54}ae_{40-56}$ with $X_{Mg} = 0.63–0.95$, and diopsidic pyroxene is $jd_{0-7}di + hd_{>94}ae_{0-20}$ with $X_{Mg} = 0.77–0.88$. No apparent difference in composition exists among different textural types of metamorphic pyroxenes. As shown in Figure 3, a single pyroxene crystal is chemically heterogeneous and does not show regular chemical zoning. The X-ray image of Al distribution shows neither systematic compositional zoning nor sector zoning. A heterogeneity—in that the Al-rich, lighter colored part (jadeite-rich) parallel to *c*-axis is intergrown with Al-poor darker portion—is recognized in the elongate grain that was cut nearly parallel to the crystallographic *c*-axis (Fig. 3A). In the crystals oblique to the *c*-axis, the compositional heterogeneity is irregular and more complex (Fig. 3B). Most Ca-Na pyroxenes in PBR show a wide compositional range within the aegirine-augite field ($jd_{0-24}di + hd_{26-80}ae_{20-67}$; $X_{Mg} = 0.65–0.95$) and overlap with those of PBC.

### *Lawsonite*

The compositions of lawsonite are plotted in Figure 6; all Fe was assumed to be $Fe^{3+}$. Lawsonite in the PBC and PBR has 0.06–0.12 $Fe^{3+}$, 1.82–1.91 Al, and 0.94–1.01 Ca p.f.u. of 8 oxygen; there was

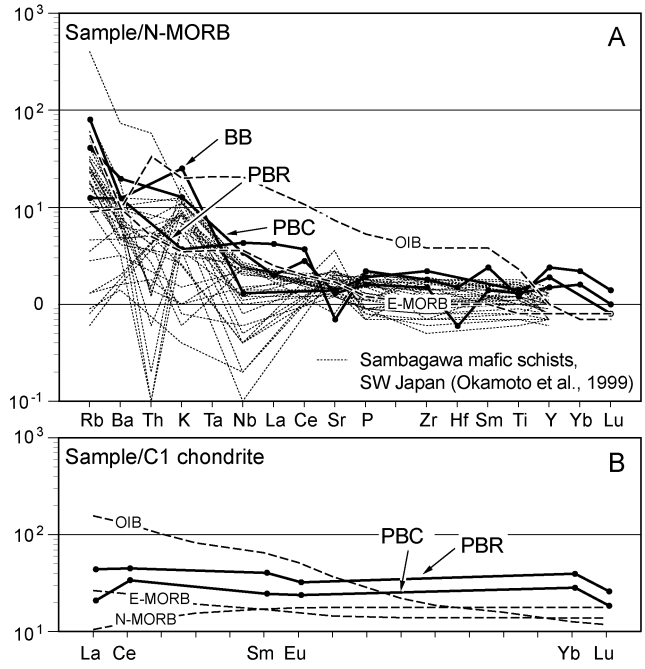


FIG. 4. Bulk-rock chemistry of the investigated samples from the Sekinomiya serpentinite body. A. N-MORB–normalized incompatible element patterns for analyzed samples of PBC, PBR, and BB. For comparison, the element abundance patterns of the mafic schist of the Sambagawa metamorphic belt, SW Japan (Okamoto and Maruyama, 1999) are shown. B. Chondrite-normalized rare-earth element (REE) patterns for PBC and PBR. Normalizing values are from Sun and McDonough (1989).

no systematic chemical zoning. In contrast, lawsonite in the BB contains a significantly lower $Fe^{3+}$ (0.02–0.06 $Fe^{3+}$ p.f.u.). Overall, lawsonite are slightly less aluminous than in lawsonite eclogites (Tsujimori et al., 2006a).

### *Chlorite*

Chlorite in the PBC and PBR has 5.6–6.0 Si, 4.3–4.7 Al, and 0.1 Mn p.f.u. of 28 oxygen. The $X_{Mg}$ values increase from PBR (0.43–0.46) to PBC (0.48–0.63) (Fig. 7).

### *Na-amphibole*

Compositions of sodic amphibole are plotted in Figure 8; the structural formulae of amphiboles were calculated based on O = 23, and the $Fe^{2+}/Fe^{3+}$ ratio was estimated with total cation = 13 excluding Ca, Na, and K. Na-amphibole in the PBR is strongly zoned; the cores are $Fe^{3+}$-rich with $Fe^{3+}/(Fe^{3+} + {}^{[6]}Al)$ = 0.61–0.74 and $X_{Mg}$ = 0.30–0.74; in contrast, the rims are mostly ferroglaucophane with $X_{Mg}$ = 0.34–0.53, and the $Fe^{3+}/(Fe^{3+} + {}^{[6]}Al)$ ratio increases from the mantle to the rims (0.10–0.44). This chemical zoning suggests Na-amphibole growth during prograde metamorphism (Liou and Maruyama, 1987). Na-amphiboles in the BB are ferroglaucophane with $X_{Mg}$= 0.33–0.45 and $Fe^{3+}/(Fe^{3+} + {}^{[6]}Al)$ = 0.05–0.37; the $X_{Mg}$ value overlaps with that of the PBR, but the minimum $Fe^{3+}/(Fe^{3+} + {}^{[6]}Al)$ ratio (0.05) is significantly lower than rim compositions of the PBR.

### *Pumpellyite*

Pumpellyite in PBR and BB is Al-rich, with Al/(Al+Fe+Mg) = 0.65–0.86 (Fig. 9). Such Al-rich pumpellyite is common among blueschist-facies rocks (e.g., Maruyama and Liou, 1988). Pumpellyite in PBR is less magnesian ($X_{Mg}$ = 0.15–0.16) than in the BB ($X_{Mg}$ = 0.51–0.55).

### *Other minerals*

Phengite is Si-rich, containing 3.55–3.65 p.f.u. for O = 11. Relict igneous augite contains 0.4–0.9 wt% $TiO_2$, 2.4–3.6 wt% $Al_2O_3$, and 0.3–0.6 wt% $Cr_2O_3$; the $X_{Mg}$ ranges from 0.78 to 0.91.

TABLE 2. Representative Electron-Microprobe Analyses of Rock-Forming Minerals in the Investigated Samples

| | Meta-pillow basalt core (PBC) | | | | | Meta-pillow basalt rim (PBR) | | | | Meta-basaltic breccia (BB) | | | | | |
|---|---|---|---|---|---|---|---|---|---|---|---|---|---|---|---|
| | Ca-Na-px | | Lws | Chl | r. Cpx | Na-amp | | Pmp | Lws | Na-amp | Pmp | Lws | Chl | Phe | r. Cpx |
| | | | | | | core | rim | | | | | | | | |
| $SiO_2$ | 53.85 | 53.60 | 38.14 | 28.05 | 52.77 | 56.88 | 55.88 | 36.69 | 38.61 | 56.66 | 36.55 | 38.73 | 26.72 | 53.35 | 51.89 |
| $TiO_2$ | 0.11 | 0.13 | 0.20 | 0.00 | 0.52 | 0.00 | 0.05 | 0.15 | 0.09 | 0.03 | 0.03 | 0.21 | 0.09 | 0.01 | 0.56 |
| $Al_2O_3$ | 5.42 | 3.82 | 29.99 | 17.89 | 2.78 | 10.13 | 4.34 | 21.99 | 30.20 | 9.50 | 22.62 | 30.90 | 17.98 | 22.74 | 2.24 |
| $Cr_2O_3$ | 0.01 | 0.00 | 0.04 | 0.00 | 0.30 | 0.00 | 0.02 | 0.04 | 0.00 | 0.01 | 0.00 | 0.00 | 0.00 | 0.00 | 0.21 |
| $Fe_2O_3$[1] | | | 2.65 | | | | | | 2.67 | | | 0.72 | 29.80 | | 7.10 |
| FeO[2] | 17.78 | 18.16 | | 26.62 | 6.56 | 17.11 | 23.70 | 6.45 | | 18.17 | 8.02 | | | 3.80 | |
| MnO | 0.10 | 0.108 | 0.03 | 0.56 | 0.19 | 0.16 | 0.10 | 0.46 | 0.10 | 0.12 | 0.54 | 0.00 | 0.52 | 0.05 | 0.28 |
| MgO | 3.54 | 4.58 | 0.05 | 16.18 | 16.97 | 6.27 | 6.52 | 3.02 | 0.18 | 5.86 | 1.72 | 0.00 | 12.77 | 4.11 | 15.94 |
| CaO | 6.84 | 8.35 | 17.02 | 0.07 | 19.20 | 0.43 | 0.56 | 21.79 | 17.46 | 0.44 | 21.93 | 17.72 | 0.07 | 0.00 | 19.59 |
| $Na_2O$ | 10.32 | 9.42 | 0.00 | 0.00 | 0.69 | 7.03 | 6.94 | 0.12 | 0.00 | 7.21 | 0.13 | 0.01 | 0.00 | 0.04 | 0.34 |
| $K_2O$ | 0.01 | 0.00 | 0.01 | 0.00 | 0.00 | 0.01 | 0.01 | 0.01 | 0.01 | 0.02 | 0.00 | 0.01 | 0.00 | 10.74 | 0.00 |
| Total | 97.99 | 98.16 | 88.12 | 89.37 | 99.97 | 98.02 | 98.12 | 90.71 | 89.30 | 98.00 | 91.54 | 88.29 | 87.94 | 94.85 | 98.14 |
| O= | 6 | 6 | 8 | 28 | 11 | 23 | 23 | 24.5 | 8 | 23 | 24.5 | 8 | 28 | 11 | 6 |
| Si | 1.996 | 1.994 | 2.021 | 5.833 | 1.927 | 7.984 | 8.012 | 6.145 | 2.017 | 8.014 | 6.113 | 2.035 | 5.762 | 3.597 | 1.945 |
| Ti | 0.003 | 0.003 | 0.008 | 0.000 | 0.014 | 0.000 | 0.005 | 0.018 | 0.003 | 0.003 | 0.004 | 0.008 | 0.014 | 0.001 | 0.016 |
| Al | 0.237 | 0.168 | 1.873 | 4.385 | 0.119 | 1.675 | 0.733 | 4.341 | 1.859 | 1.584 | 4.460 | 1.914 | 4.570 | 1.807 | 0.099 |
| Cr | 0.000 | 0.000 | 0.002 | 0.000 | 0.009 | 0.000 | 0.002 | 0.005 | 0.000 | 0.001 | 0.000 | 0.000 | 0.000 | 0.000 | 0.006 |
| $Fe^{3+}$ | 0.507 | 0.516 | 0.106 | | 0.000 | 0.313 | 1.127 | | 0.117 | 0.269 | | 0.029 | | | |
| $Fe^{2+}$ | 0.045 | 0.049 | | 4.629 | 0.201 | 1.695 | 1.714 | 0.903 | | 1.880 | 1.122 | | 5.375 | 0.214 | 0.223 |
| Mn | 0.003 | 0.003 | 0.001 | 0.099 | 0.006 | 0.019 | 0.012 | 0.066 | 0.004 | 0.014 | 0.076 | 0.000 | 0.096 | 0.003 | 0.009 |
| Mg | 0.196 | 0.254 | 0.004 | 5.013 | 0.924 | 1.313 | 1.394 | 0.754 | 0.014 | 1.235 | 0.428 | 0.000 | 4.106 | 0.413 | 0.890 |
| Ca | 0.272 | 0.333 | 0.966 | 0.016 | 0.751 | 0.064 | 0.086 | 3.911 | 0.977 | 0.066 | 3.930 | 0.998 | 0.015 | 0.000 | 0.787 |
| Na | 0.742 | 0.679 | 0.000 | 0.000 | 0.049 | 1.914 | 1.930 | 0.038 | 0.000 | 1.978 | 0.042 | 0.001 | 0.000 | 0.005 | 0.024 |
| K | 0.000 | 0.000 | 0.001 | 0.000 | 0.000 | 0.001 | 0.002 | 0.003 | 0.001 | 0.003 | 0.000 | 0.000 | 0.000 | 0.924 | 0.000 |
| Total | 4.000 | 4.000 | 4.981 | 19.975 | 4.000 | 14.979 | 15.018 | 16.184 | 4.992 | 15.047 | 16.175 | 4.986 | 19.939 | 6.964 | 3.999 |

[1]Total Fe as $Fe_2O_3$.
[2]Total Fe as FeO.

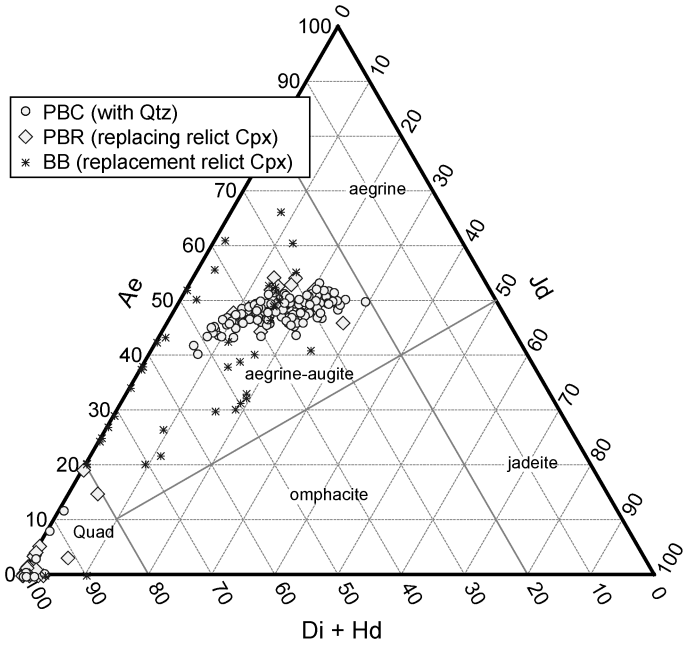


FIG. 5. Compositional variations of clinopyroxene in PBC and PBR from the Sekinomiya serpentinite body. Abbreviations: jd = jadeite; ae = aegirine; di + hd = diopside and hedenbergite; Quad = Ca-Mg-Fe pyroxenes.

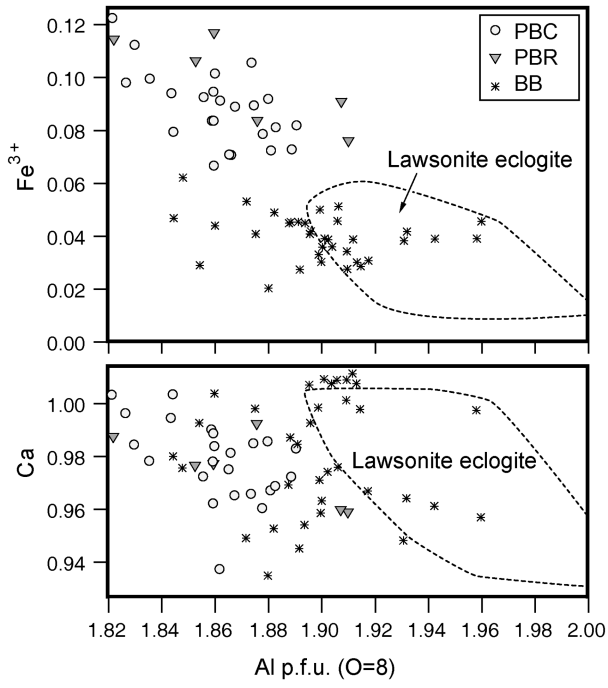


FIG. 6. Compositional variations of lawsonite in PBC, PBR, and BB from the Sekinomiya serpentinite body. The dashed line delineates compositional fields of lawsonite from Guatemalan lawsonite eclogites and related HP-LT rocks.

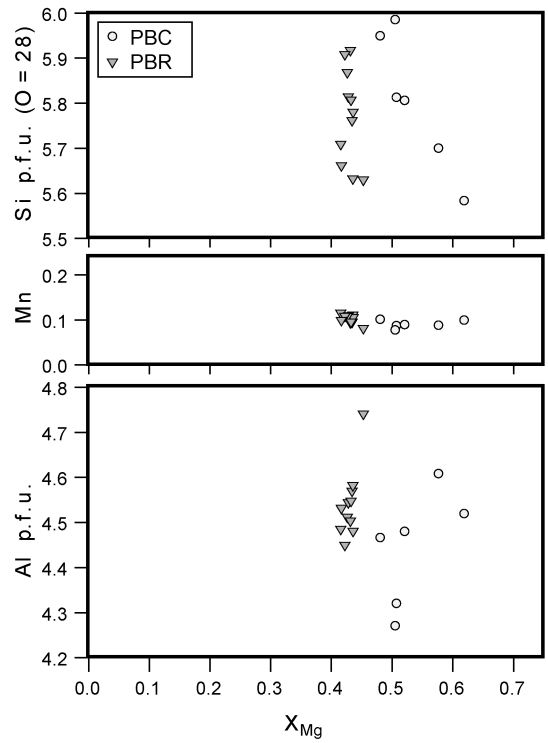


FIG. 7. Compositional variations of chlorite in PBC and BB from the Sekinomiya serpentinite body.

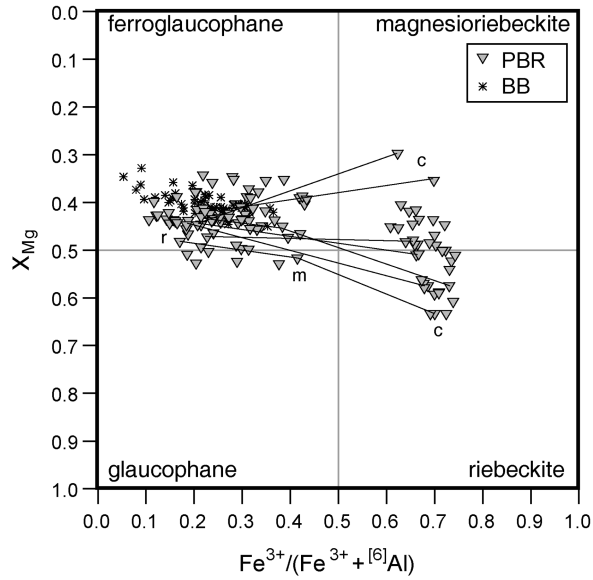


FIG. 8. Compositional variations of Na-amphibole in PBC and PBR from the Sekinomiya serpentinite body.

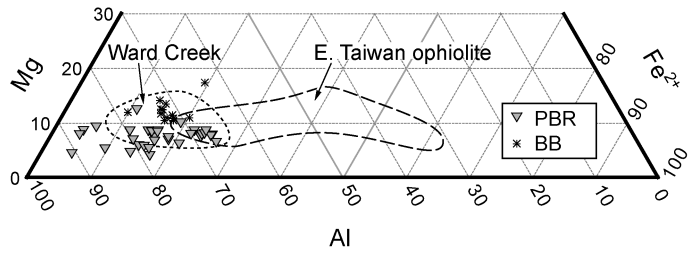


FIG. 9. Compositional variations of pumpellyite in PBR and BB from the Sekinomiya serpentinite body. Compositional fields of pumpellyite from the Ward Creek blueschist (Maruyama and Liou, 1988) and East Taiwan ophiolite (Liou, 1979) are also shown.

## P-T Conditions of Metamorphism

Metamorphic conditions of the investigated samples were estimated based on available phase equilibria. The presence of pumpellyite and absence of epidote in the PBR and BB suggest that the maximum T of metamorphism is limited by the experimentally determined reaction: Mg-Al Pmp = Czo + Grs + Chl + Qtz + $H_2O$ (Schiffman and Liou, 1980). Furthermore, the generic petrogenetic grids in the system $Na_2O$–CaO–MgO–$Al_2O_3$–$SiO_2$–$H_2O$ imply that the Na-amp + Lws and Na-amp + Pmp assemblages in the PBR and BB are stable at higher P and lower T than the pumpellyite-actinolite facies; they can be described as lawsonite-blueschist facies (e.g., Evans, 1990; Frey et al., 1991; Banno, 1998; Katzir et al., 2000). The reaction: 17 Gln + 24 Lws = 6 Pmp + 9 Chl + 19 Qtz + 34 Ab + 8 $H_2O$ (Katzir et al., 2000) constrains the approximate P = 0.7 GPa at T = ~300°C for the Na-amp-bearing mineral assemblages of PBR and BB. The presence of Si-rich phengite (up to 3.65 p.f.u.) also suggests high-P and low-T conditions (Velde, 1967; Massonne and Schreyer, 1987). In the PBC, the Ca-Na px (maximum Jd = 29%) + Qtz assemblage yields a P > 0.65 GPa at T = 280 °C (Holland, 1983). In very low-T blueschist-facies metamorphism, the Ca-Na px + Lws + Chl assemblage has been described in metabasalts from several localities (e.g., Okay, 1982; Hirajima, 1984; Sakakibara, 1991). Hirajima (1983) calculated a Schreinemakers' grid showing the stability field of diopside (Di) + Lws + Chl at blueschist-facies conditions. The Ca-Na px + Lws + Chl assemblage in our PBC may have formed at the P-T conditions of his Di + Chl + Lws field. Sakakibara (1991) described the Ca-Na px + Lws + Pmp + Chl assemblage from Tokoro metabasalts of Hokkaido, Japan, and estimated T = 200–230°C at 0.6 GPa. Because many petrologic similarities exist between the investigated PBC and the "Lw-Napx zone" metabasalts of Sakakibara (1990), the investigated samples may record blueschist-facies conditions similar to those of Tokoro metabasalts.

## Discussion

### *Na-Ca pyroxene–lawsonite–chlorite assemblage in low-grade metamorphism*

In the investigated samples, the PBC differs from the PBR and BB in its lack of Na-amphibole. Although these rocks differ in mineral assemblages, they may have recrystallized at the same P-T conditions; the appearance of different assemblages may be mainly controlled by bulk-rock compositions, as illustrated below.

The mineral parageneses of the investigated meta-mafic rocks can be discussed in terms of a four-component system Ca (CaO-$TiO_2$)–2Al ($Al_2O_3$-$Na_2O$-0.87$K_2O$) – 2$Fe^{3+}$ ($Fe_2O_3$) – *R* (FeO + MgO – 0.345$K_2O$) after Maruyama et al. (1985) (Fig. 10). We assume that: (1) $K_2O$ and $TiO_2$ are present only in phengite [$K_2Al_{1.74}R_{0.65}Si_{3.57}O_{10}(OH)_2$] and titanite, respectively; (2) quartz and albite are excess phases; (3) the fluid phase consists of pure $H_2O$ and is treated as an excess phase; and (4) FeO and MgO are exchangeable. In this system, parageneses of minerals are graphically represented as invariant points, univariant lines, divariant planes, and trivariant tetrahedrons within a tetrahedron with Ca-2Al-2$Fe^{3+}$-*R* at its apices (Fig. 10A). Assuming albite as an excess phase in the PBC, the Ca-Na px + Lws + Chl assemblage plane can coexist within a Na-amp + Lws + Pmp + Chl tetrahedron. In other words, lack of Na-amphibole in the PBC is not due to retrogression. Moreover, the Ca-Na px + Lws +

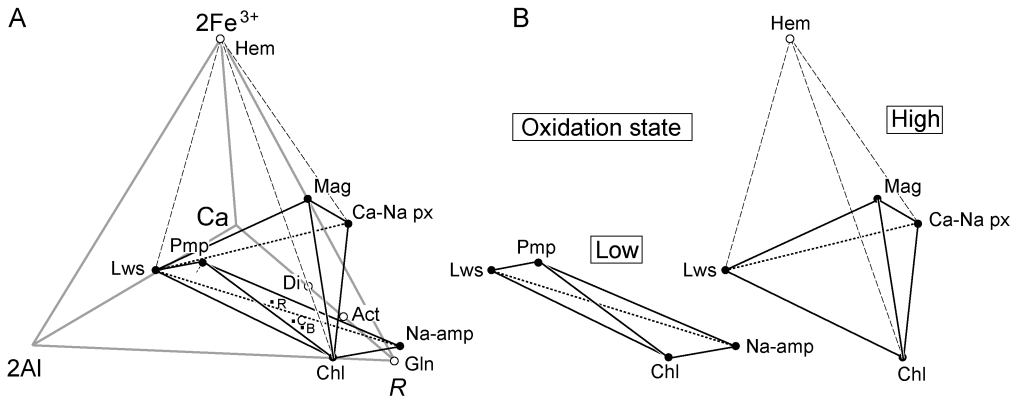


FIG. 10. Phase relations observed in the investigated rocks in the Ca-2Al-2Fe$^{3+}$-*R* tetrahedron. A. The Ca-2Al-2Fe$^{3+}$-*R* tetrahedron showing blueschist-greenschist minerals. Filled circles represents observed mineral assemblages. Bulk-rock compositions of each sample are also drawn as small filled squares on the 2Al-2Fe$^{3+}$-*R* plane. Abbreviations: C = meta-pillow basalt core; R = meta-pillow basalt rim; B = meta-basaltic breccia. B. Tetrahedrons showing observed mineral assemblages.

Chl (+ Mag or + Hem) assemblage requires a bulk-rock composition richer in $Fe^{3+}$ than that of the Na-amp + Lws + Pmp + Chl assemblage. This suggests that a relatively high oxidation state is necessary to form the Ca-Na px + Lws + Chl assemblage. Moreover, the presence of Ca-Na pyroxene in quartz-lawsonite veins suggests fluid infiltration promoted the crystallization of Ca-Na px + Lws + Chl mineral assemblage.

de Roever (1972) proposed the lawsonite-albite sub-facies in a P-T field just below the blueschist facies, in which Lws + Chl +Ab is stable instead of Na-amp, also described as "lawsonite-chlorite facies" (e.g., Turner, 1981; Peacock, 1993). The high-pressure limit of the lawsonite-chlorite facies is defined by the reaction: 5 Gln + 2 Lws = Tr + 10 Ab + 2 Chl. This reaction does not involve $H_2O$, and its P-T equilibrium curve is thus independent of fluid pressure.

According to this reaction, however, the appearance of Na-amphibole requires an initial mineral assemblage containing Ca-amphibole. Although the Ca-Na px + Lws + Chl assemblage in PBC might have been in equilibrium with lawsonite-blueschist–facies P-T conditions, the lack of Na-amphibole might be due to that the absence of Ca-amphibole from the initial mineral assemblage. This is consistent with the fact that actinolitic amphibole is not common in hydrothermally altered pillow basalts in the modern ocean floor (e.g., Alt and Teagle, 2000).

### *Significance of the Ca-Na px + Lws + Chl assemblage as a possible precursor of the lawsonite eclogitic mineral assemblage*

The transformation from blueschist to eclogite is one of the most characteristic reactions in the subduction-zone process (e.g., Peacock, 1993; Maruyama et al., 1996; Ernst, 2005). Minor prograde blueschist-facies minerals are preserved in glaucophane-epidote eclogites (e.g., Clarke et al., 1997; Gao et al., 1999; Tsujimori, 2002) as inclusions of porphyroblastic garnets. Considering those natural occurrences, it is likely that epidote-blueschist or lawsonite-blueschist transforms to glaucophane-epidote eclogite by various dehydration reactions. In other words, blueschist is a major precursor of glaucophane-epidote eclogite. However, the precursor assemblage for lawsonite eclogite is not well known because lawsonite eclogite is not common.

Basaltic lawsonite eclogites contain a characteristic Grt + Omp + Lws assemblage (cf., Tsujimori et al., 2006b). In Guatemalan lawsonite eclogites, prograde glaucophane is less common within porphyroblastic garnet; instead chlorite and pumpellyite occur as prograde inclusions (Tsujimori et al., 2006a). Moreover, lawsonite xenoliths in kimberlitic pipes at Garnet Ridge in the Colorado Plateau also lack Na-amphibole in prograde-zoned garnet (Usui et al., 2006). If we consider that chlorite decomposes to produce garnet with increasing

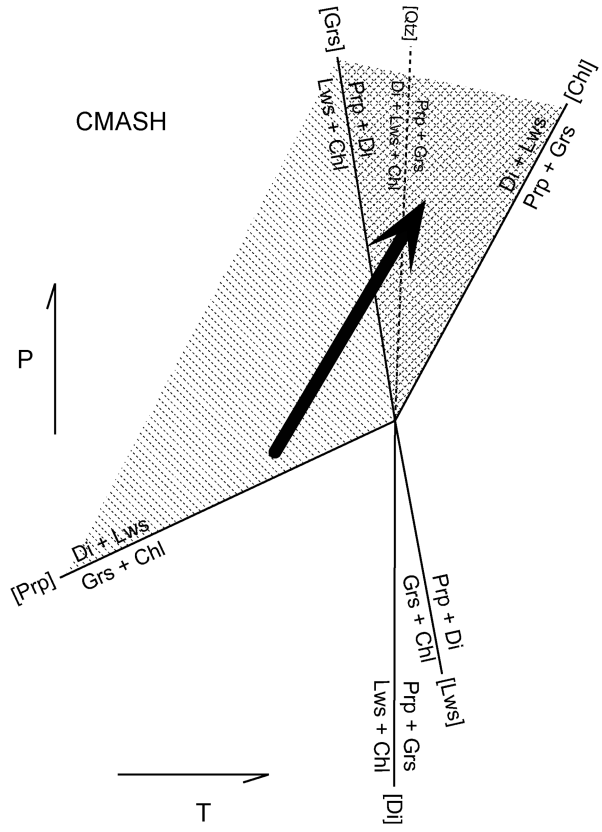


FIG. 11. Schreinemakers' grids in P-T space. The invariant points and univariant reactions are calculated by the BEYES version 1.1 program with an internally consistent thermodynamic dataset (Chatterjee et al., 1998). The grey area represents the Di (= Ca-Na px) + Lws + Chl assemblage in low-T blueschist-facies metabasalts. The hatched area represents lawsonite eclogite mineral assemblage of Prp (= Grt) + Di (= Omp) + Lws. Arrow represents a possible prograde P-T path of lawsonite eclogite.

pressure and temperature, the Ca-Na px + Lws + Chl assemblage in low-T blueschist-facies metabasalts appears to be the most suitable candidate for the precursor mineral assemblage of lawsonite eclogite. A simple phase relationship among lawsonite, chlorite, diopside, pyrope, and grossular in the CaO-$Al_2O_3$-MgO-$SiO_2$-$H_2O$ system is shown in Figure 11. In this Schreinemakers' grid, the Prp (= Grt) + Di (= Omp) + Lws stability field represents lawsonite eclogite. During subduction, incipiently metamorphosed ocean-floor basalts containing the Di (= Ca-Na px) + Lws + Chl assemblage might continuously transform to the Grt + Omp + Lws mineral assemblage with increasing P and T (Fig. 11). Okay (1982) described grossular-rich garnet in a Ca-Na pyroxene- and lawsonite-bearing metabasalt of the Tavşanli region of northwestern Turkey. The invariant reaction 5 Di + 4 Lws = 3 Grs + Chl + 6 Qtz suggests that the grossular-rich garnet can coexist with the Ca-Na px + Lws assemblage at lower values of P and T. Recently, Tsujimori et al. (2006a) suggested lawsonite eclogitization was initiated at T = ~300°C and the chlorite-consuming reaction to form Fe–Mg–Mn garnet is more effective than the lawsonite-consuming reaction to form grossular component. During incipient eclogitization, Ca-Na pyroxene might change compositions to omphacite or jadeite by consuming albite. Furthermore, chlorite might be continuously consumed to form garnet, similar to the case of the garnet-forming reaction in the pelitic system proposed by Inui and Toriumi (2004).

As mentioned above, the Ca-Na px + Lws + Chl assemblage is stable at a relatively high oxidation

state. In general, the degree of oxidation of oceanic crust increases through reaction with seawater-derived hydrothermal fluids near the spreading center and oxygenated deep-sea water (e.g., Alt, 1995). Bach and Edwards (2003) and Edwards et al. (2004) suggested that the average oxidation state of upper basaltic ocean crust increases with time through microbial Fe-oxidation; in other words, older oceanic crust is more intensely altered and oxidized. If so, the Ca-Na px + Lws + Chl assemblage rather than Na-amphibole–bearing mineral assemblage may be favorable for such oxidized oceanic crust. The subduction of old oceanic crust is crucial to the formation of a "cold" subduction-zone geotherm (e.g., Peacock, 1993; Peacock and Wang, 1999). We propose that the subduction of old oceanic crust first produces the Ca-Na px + Lws + Chl assemblage by fluid infiltration in a cold subduction zone at shallow depths, and then the fully hydrated metabasalts with the Na-amphibole–free mineral assemblage continuously transform to lawsonite eclogite below 300°C at greater depths. In essence, the Ca-Na px + Lws + Chl assemblage is a low-T equivalent of the lawsonite eclogite mineral assemblage.

## Acknowledgments

This research was supported by the Japanese Society for the Promotion of Science, through a Research Fellowship for Research Abroad for the first author (Tsujimori) and the National Science Foundation through NSF grant EAR-0510325 (Liou). We thank A. Ishiwatari, H. Ishida, H. Shukuno, and M. Motoya for helping with the XRF and INNA analyses and T. Itaya for providing the facility for the EMP analyses. We thank C. G. Mattinson and W. G. Ernst for critically reviewing this manuscript.

## REFERENCES

Alt, J. C., 1995, Sub-seafloor processes in mid-ocean ridge hydrothermal systems, *in* Humphris, S. E., Zierenberg, R. A., Mullineaux, L. S., and Thomson, R. E., eds., Seafloor hydrothermal systems: Washington, DC, American Geophysical Union, p. 85–114.

Alt, J. C., and Teagle D. A. H., 2000, Hydrothermal alteration and fluid fluxes in ophiolites and oceanic crust, *in* Dilek, Y., Moores, E., Elthon, D., and Nicolas, A. eds., Ophiolites and oceanic crust: New insights from field studies and the Ocean Drilling Program: Geological Society of America Special Publication 349, p. 273–282.

Bach, W., and Edwards, K. J., 2003, Iron and sulfide oxidation within the basaltic ocean crust: Implications for chemolithoautotrophic microbial biomass production: Geochimica et Cosmochimica Acta, v. 67, p. 3871–3887.

Banno, S., 1998, Pumpellyite-actinolite facies of the Sanbagawa metamorphism: Journal of Metamorphic Geology, v. 16, p. 117–128.

Chatterjee, N. D., Krüger, R., Haller, G., and Olbricht, W., 1998, The Bayesian approach to an internally consistent thermodynamic database: Theory, database, and generation of phase diagrams: Contributions to Mineralogy and Petrology, v. 133, p. 149–168.

Clarke, G. L., Aitchison, J. C., and Cluzel, D., 1997, Eclogites and blueschists of the Pam Peninsula, NE New Caledonia: A reappraisal: Journal of Petrology, v. 38, p. 843–876.

de Roever, E. W. F., 1972, Lawsonite-albite facies metamorphism near Fuscaldo, Calabria (southern Italy), its geological significance and petrological aspects: Ph.D thesis, University of Amsterdam, Amsterdam, GUA Papers of Geology, Series 1, 163 p.

Edwards, K. J., Bach, W., McCollom, T. M., and Rogers, D. R., 2004, Neutrophilic iron-oxidizing bacteria in the ocean: Their habitats, diversity, and roles in mineral deposition, rock alteration, and biomass production in the deep-sea: Geomicrobiology Journal, v. 21, p. 393–404.

Ernst, W. G., 2005, Alpine and Pacific styles of Phanerozoic mountain building: Subduction-zone petrogenesis of continental crust: Terra Nova, v. 17, p. 165–188.

Evans, B. W., 1990, Phase-relations of epidote-blueschists: Lithos, v. 25, p. 3–23.

Frey, M., Decapitani, C., and Liou, J. G., 1991, A new petrogenetic grid for low-grade metabasites: Journal of Metamorphic Geology, v. 9, p. 497–509.

Gao, J., Klemd, R., Zhang, L., Wang, Z., and Xiao, X., 1999, P-T path of high-pressure/low-temperature rocks and tectonic implications in the western Tianshan Mountains, NW China: Journal of Metamorphic Geology, v. 17, p. 621–636.

Hacker, B. R., Abers, G. A., and Peacock, S. M., 2003, Subduction factory—1. Theoretical mineralogy, densities, seismic wave speeds, and $H_2O$ contents: Journal of Geophysical Research–Solid Earth, v. 108, p. 20–29.

Harlow, G. E., 1999, Interpretation of Kcpx and CaEs components in clinopyroxene from diamond inclusions and mantle samples, *in* Gurney, J. J. Gurney, J. L., Pascoe, M. D., and Richardson, S. H., eds., Proceedings of Seventh International Kimberlite Convention, v. I: Cape Town, South Africa, p. 321–331.

Hashimoto, M., and Igi, S., 1970, Finding of lawsonite-glaucophane schists from the Sangun metamorphic terranes of eastern Chugoku province: Journal of

Geological Society of Japan, v. 76, p. 159–160 (in Japanese).

Hirajima, T., 1983, The analysis of the paragenesis of glaucophanitic metamorphism for a model ACF system by Schreinemakers' method: Journal of Geological Society of Japan, v. 89, p. 679–691.

Hirajima, T., 1984, The greenrock melange in the Yorii area in the northeastern part of the Kanto Mountains: Journal of Geological Society of Japan, v. 89, p. 629–642.

Holland, T. J. B., 1983, The experimental determination of activities in disordered and short-range ordered jadeitic pyroxenes: Contributions to Mineralogy and Petrology, v. 82, p. 214–220.

Inui, M., and Toriumi, M., 2004, A theoretical study on the formation of growth zoning in garnet consuming chlorite: Journal of Petrology, v. 45, p. 1369–1392.

Ishiwatari, A., and Hayasaka, Y., 1992, Ophiolite nappes and blueschists of the Inner Zone of Southwest Japan, *in* 29th International Geological Congress Field Trip C22 Guide Book, v. 5: Tsukuba, Japan, Geological Survey of Japan, p. 285–326.

Ishiwatari, A., and Tsujimori, T., 2003, Paleozoic ophiolites and blueschists in Japan and Russian Primorye in the tectonic framework of East Asia: A synthesis: Island Arc, v. 12, p. 190–206.

Isozaki, Y., 1997, Jurassic accretion tectonics of Japan: Island Arc, v. 6, p. 25–51.

Katzir, Y., Avigad, D., Matthews, A., Garfunkel, Z., and Evans, B.W., 2000, Origin, HP/LT metamorphism, and cooling of ophiolitic mélanges in southern Evia (NW Cyclades), Greece: Journal of Metamorphic Geology, v. 18, p. 699–718.

Kretz, R., 1983, Symbols for rock-forming minerals: American Mineralogist, v. 68, p. 277–279.

Liou, J. G., 1971, P-T stabilities of laumontite, wairakite, lawsonite, and related minerals in system $CaAl_2Si_2O_8$-$SiO_2$-$H_2O$: Journal of Petrology, v. 12, p. 378–411.

Liou, J. G., 1979, Zeolite facies metamorphism of basaltic rocks from the East Taiwan Ophiolite: American Mineralogist, v. 64, p. 1–14.

Liou, J. G., and Maruyama, S., 1987, Parageneses and compositions of amphiboles from Franciscan jadeite glaucophane type facies series metabasites at Cazadero, California: Journal of Metamorphic Geology, v. 5, p. 371–395.

Maruyama, S., and Liou, J. G., 1985, The stability of Ca-Na pyroxene in low-grade metabasites of high-pressure intermediate facies series: American Mineralogist, v. 70, p. 16–29.

Maruyama, S., and Liou, J. G., 1988, Petrology of Franciscan metabasites along the jadeite-glaucophane type facies series, Cazadero, California: Journal of Petrology, v. 29, p. 1–37.

Maruyama, S., and Liou, J. G., 2005, From snowball to Phanerozoic Earth: International Geology Review, v. 47, p. 775–791.

Maruyama, S., Liou, J. G., and Sakakura, Y., 1985, The stability of Ca-Na pyroxene in low-grade metabasites of high-pressure intermediate facies series: American Mineralogist, v. 70, p. 16–29.

Maruyama, S., Liou, J. G., and Terabayashi, M., 1996, Blueschists and eclogites of the world and their exhumation: International Geology Review, v. 38, p. 485–594.

Massonne, H. J., and Schreyer, W., 1987, Phengite geobarometry based on the limiting assemblage with K-feldspar, phlogopite, and quartz: Contributions to Mineralogy and Petrology, v. 96, p. 212–224.

Nishimura, Y., 1998, Geotectonic subdivision and areal extent of the Sangun belt, Inner Zone of Southwest Japan: Journal of Metamorphic Geology, v. 16, p. 129–140.

Nitsch, K. H., 1968, Die Stabilität von Lawsonit: Naturwissenschaften, v. 55, p. 388.

Okamoto, K., and Maruyama, S., 1999, The high-pressure synthesis of lawsonite in the MORB+$H_2O$ system: American Mineralogist, v. 84, p. 362–373.

Okay, A. I., 1982, Incipient blueschist metamorphism and metasomatism in the Tavşanli region, northwest Turkey: Contributions to Mineralogy and Petrology, v. 79, p. 361–367.

Ohtani, E., 2005, Water in the mantle. Elements, v. 1, p. 25–30.

Pawley, A. R., 1994, The pressure and temperature stability limits of lawsonite—implications for $H_2O$ recycling in subduction zones: Contributions to Mineralogy and Petrology, v. 118, p. 99–108.

Peacock, S. M., 1993, The importance of blueschist-eclogite dehydration reactions in subducting oceanic crust: Geological Society of America Bulletin, v. 105, p. 684–694.

Peacock, S. M., and Wang, K., 1999, Seismic consequences of warm, versus cool subduction metamorphism: Examples from southwest and northeast Japan: Nature, v. 286, p. 937–939.

Pearce, J. A., 1982, Trace element characteristics of lavas from destructive plate bounders, *in* Thorpe, R. S., ed., Andesites: Orogenic andesites and related rocks: New York, NY, John Wiley and Sons, Inc., p. 525–548.

Pearce, J. A., 1983, The role of sub-continental lithosphere in magma genesis at distractive plate margins, *in* Hawkesworth, C. J., and Norry, M. J., eds., Continental basalts and mantle xenoliths: Nantwich, UK, Shiva Publ., p. 230–249.

Sakakibara, M., 1991, Metamorphic petrology of the northern Tokoro metabasites, eastern Hokkaido, Japan: Journal of Petrology, v. 32, p. 333–364.

Schmidt, M. W., 1995, Lawsonite: Upper pressure stability and formation of higher density hydrous phases: American Mineralogist, v. 80, p. 1286–1292.

Schiffman, P., and Liou, J. G., 1980, Synthesis and stability relations of Mg-Al pumpellyite, $Ca_4Al_5MgSi_6O_{21}(OH)_7$: Journal of Petrology, v. 21, p. 414–474.

Schmidt, M. W., and Poli, S., 1994, The stability of lawsonite and zoisite at high pressure: Experiments in CASH to 92 kbar and implications for the presence of hydrous phases in subducted lithosphere: Earth and Planetary Science Letters, v. 124, p. 105–118.

Schmidt, M. W., and Poli, S., 1998, Experimentally based water budgets for dehydrating slabs and consequences for arc magma generation: Earth and Planetary Science Letters, v. 163, p. 361–379.

Sun, S. S., and McDonough, W. E., 1989, Chemical and isotopic systematics of ocean basalts: Implications for mantle composition and processes, *in* Saunders, A. D. and Norry, M. J., eds., Magmatism in the ocean basins: Oxford, UK: Blackwell Scientific, Geological Society Special Publication, p. 313–345.

Snow, C. A., 2006, A re-evaluation of tectonic discrimination diagrams and a new probabilistic approach using large geochemical databases: Moving beyond binary and ternary plots: Journal of Geophysical Research–Solid Earth, in press.

Tazaki, K., and Ishiuchi, K., 1976, Coexisting jadeite and paragonite in albitite: Journal of the Mineralogical Society of Japan, v. 12, p. 184–194 (in Japanese).

Tsujimori, T., 1997, Omphacite-diopside vein in an omphacitite block from the Osayama serpentinite melange, Sangun-Renge metamorphic belt, southwestern Japan: Mineralogical Magazine, v. 61, p. 845–852.

Tsujimori, T., 1998, Geology of the Osayama serpentinite melange in the central Chugoku Mountains, southwestern Japan: 320 Ma blueschist-bearing serpentinite melange beneath the Oeyama ophiolite: Journal of the Geological Society of Japan, v. 104, p. 213–231 (in Japanese with English abstract).

Tsujimori, T., 2002, Prograde and retrograde P-T paths of the late Paleozoic glaucophane eclogite from the Renge metamorphic belt, Hida Mountains, southwestern Japan: International Geology Review, v. 44, p. 797–818.

Tsujimori, T., and Itaya, T., 1999, Blueschist-facies metamorphism during Paleozoic orogeny in southwestern Japan: Phengite K-Ar ages of blueschist-facies tectonic blocks in a serpentinite melange beneath early Paleozoic Oeyama ophiolite: Island Arc, v. 8, p. 190–205.

Tsujimori, T., and Liou, J. G., 2004, Coexisting chromian omphacite and diopside in tremolite schist from the Chugoku Mountains, SW Japan: The effect of Cr on the omphacite-diopside immiscibility gap: American Mineralogist, v. 89, p. 7–14.

Tsujimori, T., and Liou, J. G., 2005a, Eclogite-facies mineral inclusions in clinozoisite from Paleozoic blueschist, central Chugoku Mountains, southwest Japan: Evidence of regional eclogite-facies metamorphism: International Geology Review, v. 47, p. 215–232.

Tsujimori, T., and Liou, J. G., 2005b, Low-pressure and low-temperature K-bearing kosmochloric diopside from the Osayama serpentinite melange, SW Japan: American Mineralogist, v. 90, p. 1629–1635.

Tsujimori, T., Liou, J. G., Wooden, J. L., and Miyamoto, T., 2005, U-Pb dating of large zircons in low-temperature jadeitite from the Osayama serpentinite melange, Southwest Japan: Insights into the timing of serpentinization: International Geology Review, v. 47, p. 1048–1057.

Tsujimori, T., Sisson, V. B., Liou, J. G., Harlow, G. E., and Sorensen, S. S., 2006a, Petrologic characterization of Guatemalan lawsonite eclogite: Eclogitization of subducted oceanic crust in a cold subduction zone, *in* Hacker, B. R., McClelland, W. C., and Liou, J. G., eds., Ultrahigh-pressure metamorphism: Deep continental subduction: Geological Society of America Special Paper 403, p. 147–168.

Tsujimori, T., Sisson, V. B., Liou, J. G., Harlow, G. E., and Sorensen, S. S., 2006b, Very low temperature record in subduction process: A review of worldwide lawsonite eclogites: Lithos [doi: 10.1016/j.lithos.2006.03.054].

Turner, F. J., 1981, Metamorphic petrology: Mineralogical, field, and tectonic aspects: New York, NY, McGraw-Hill, 524 p.

Usui, T., Nakamura, E., and Helmstaedt, H. H., 2006. Petrology and geochemistry of eclogite xenoliths from the Colorado Plateau: Implications for the evolution of the subducted oceanic crust: Journal of Petrology, v. 47, p. 929–964.

Usui, T., Nakamura, E., Kobayashi, K., and Maruyama, S., 2003, Fate of the subducted Farallon plate inferred from eclogite xenoliths in the Colorado Plateau: Geology, v. 31, p. 589–592.

Velde, B., 1967, Phengite micas—synthesis, stability, and natural occurrence: American Journal of Science, v. 263, p. 886–913.

Vermeesch, P., 2006a, Tectonic discrimination of basalts with classification trees: Geochimica et Cosmochimica Acta, v. 70, p. 1839–1848.

Vermeesch, P., 2006b, Tectonic discrimination diagrams revisited: Geochemistry, Geophysics, and Geosystems, v. 7, Q06017 [doi: 10.1029/2005GC001092]..

Zack, T., Rivers, T., Brumm, R., and Kronz, A., 2004, Cold subduction of oceanic crust: Implications from a lawsonite eclogite from Dominican Republic: European Journal of Mineralogy, v. 16, p. 909–916.